Environmental Science & Technology Letters

pubs.acs.org/journal/estlcu

Letter

Ionic Strength and Species Drive Iron–Carbon Adsorption Dynamics: Implications for Carbon Cycling in Future Coastal Environments

E. J. Tomaszewski,* E. K. Coward, and D. L. Sparks

Cite This: *Environ. Sci. Technol. Lett.* 2021, 8, 719–724

Read Online

ACCESS | Metrics & More | Article Recommendations | Supporting Information

ABSTRACT: In coastal environments, sea level rise (SLR) will likely alter reactions between organic matter (OM) and iron (Fe) minerals. A molecular understanding of OM–Fe reactions in complex ionic matrices such as seawater is lacking. We investigated the temporal molecular composition and adsorption of coastal OM to ferrihydrite (Fh) over 24 h in low-ionic strength water (LIW) (I = 0.0009 M), mid-ionic strength water (MIW) (I = 0.003 M) (freshwater proxy), and high-ionic strength water (HIW) (I = 0.6 M) (seawater proxy). Adsorbed OM concentrations significantly ($p < 0.05$) decreased in HIW (2.12 ± 0.03 mg C/g Fh), compared to those in MIW (3.24 ± 0.56 mg C/g Fh) and LIW (3.74 ± 0.36 mg C/g Fh). In combination with adsorbed ions in HIW (9–195 mg/g Fh) compared to adsorbed ions in MIW and LIW (0.02–0.9 mg/g Fh), an ionic strength threshold is evident. This threshold effect was reflected in the dynamic molecular composition of OM, characterized via Fourier transform ion cyclotron mass spectrometry. In LIW and MIW, rapid sequential adsorption of polycyclic aromatic and phenolic compounds occurred, followed by increasing adsorption of highly unsaturated compounds. Conversely, OM in HIW did not exhibit observable selective adsorption. Overall, limited OM adsorption and indiscriminate fractionation as a result of SLR will likely impact carbon cycling.

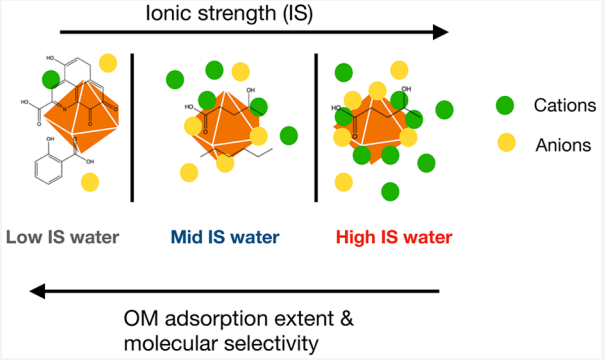

INTRODUCTION

Over the next century, global sea level rise (SLR) is expected to be between 0.2 and 1.0 m,[1,2] impacting coastal water quality and ecosystem health. Seawater has a high ionic strength (I = 0.7 M) and a high pH (8.1) compared to those of freshwater and brackish water.[3,4] These aqueous geochemical characteristics affect the solubility and surface site availability of iron (Fe) minerals, which provide important reactive surfaces for organic carbon (C) species.[5] In particular, ferrihydrite [$(Fe^{3+})_2O_3{\cdot}0.5H_2O$],[6,7] a short-range-ordered Fe (oxyhydr)-oxide with a relatively large surface area (200–600 $m^2\ g^{-1}$),[8] is a prevalent sorbent of organic matter (OM) in soil and sediment systems.[9]

The adsorption of OM to ferrihydrite leads to fractionation of organic carbon species, often marked by preferential net absorption of high-molecular weight and aromatic compounds.[9−11] However, equilibrium adsorption data present the net effect of molecular fractionation. Important temporal phenomena, such as molecular assembly, scaffolding, and exchange processes, may be lost, or concurrent processes may be difficult to disentangle. An improved understanding of the kinetic structuring of organic compounds at mineral interfaces is crucial to predicting the residence time of bound OM, as compound-specific layering or architecture may lead to disparities in C persistence from micrometer to ecosystem scales. The potential for hierarchical stabilization rates driven by position within such an architecture is not currently accounted for in model or conceptual frameworks of OM cycling.

The potential for structurally selective adsorption is particularly critical for coastal ecosystems, where SLR can impact redox-driven biogeochemical cycling and Fe-rich soil and sediment reactivity.[12−16] Mineral-phase speciation and C stabilization capacity may be substantially altered by environmental pH, eH, and ionic strength, which in turn may dictate the turnover times and composition of OM adsorbed to these Fe-bearing minerals. The impact of ionic species on Fe–OM adsorption dynamics, however, remains uncertain, largely due to the diversity of often competing, intertwined reactions and feedback processes. Ions may enhance carbon adsorption via cation bridging by up to >2-fold.[17−20] Conversely, ions may

Received: June 7, 2021
Revised: July 13, 2021
Accepted: July 15, 2021
Published: July 19, 2021

https://doi.org/10.1021/acs.estlett.1c00432
Environ. Sci. Technol. Lett. 2021, 8, 719–724

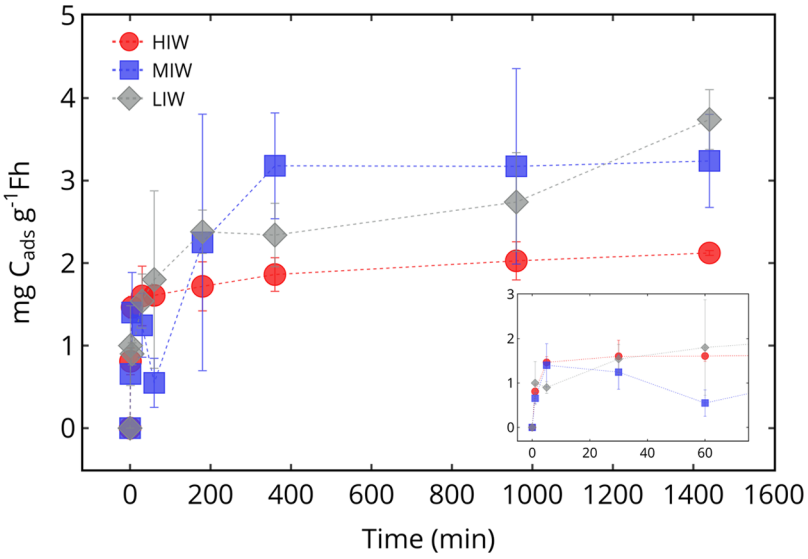

Figure 1. Concentrations of adsorbed carbon (C) in milligrams per gram of Fh, calculated from dissolved organic carbon concentrations obtained via total organic carbon analysis over the 24 h OM−ferrihydrite adsorption reaction. The different matrices used included high-ionic strength water [HIW (red circles)], mid-ionic strength water [MIW (blue squares)], or low-ionic strength water [LIW (gray diamonds)]. Error bars represent the standard deviation calculated from triplicate reactor concentrations. The inset displays data from the first 60 min of reaction.

create steric or thermodynamic constraints, i.e., via competition and co-adsorption, and inhibit adsorption through occupation of available binding sites.[20−23] Distinguishing the relative contributions of these contrasting processes, and the impact of complex ion matrices rather than the breadth of single-ion studies currently published,[18−20,24] is critical to parametrizing the role of mineral adsorption in C sequestration in coastal ecosystems. Therefore, the goal of this study was to investigate the effects of ionic strength on fractionation of estuarine dissolved OM (DOM) to ferrihydrite. By furthering our understanding of the OM fraction in complex matrices, we can better predict changes in C pools in relation to SLR and the cascading effects on other biogeochemical cycles.

MATERIALS AND METHODS

Ferrihydrite (Fh) synthesis and DOM extraction techniques are detailed in Text S1 of the Supporting Information. Three different ionic strength matrices were used in OM adsorption experiments: low (I = 0.0009 M), mid (I = 0.003 M), and high (I = 0.6 M). The matrix composition is described in Text S1. The ionic strength of the LIW matrix was empirically determined on the basis of maximum measured dissolved concentrations of Na, Mg, Ca, and S, initially associated with extracted DOM. The MIW matrix is a proxy for freshwater bodies, and the HIW matrix is a proxy for seawater; as such, there are differences in ionic composition (Text S1).

Twenty-four sacrificial reactors were prepared for each matrix/DOM solution, in which 50 mL polyethylene tubes contained 0.25 g of Fh, 40 mL of either LIW, MIW, or HIW, and 10 mL of DOM (200 mg /L) for a starting concentration of 40 mg/L. Reactors were rotated on a horizontal shaker at 250 rpm prior to temporal sacrifice after adsorption for 1, 5, 30, 60, 180, 360, 960, and 1440 min between Fh and DOM, in accordance with previous work.[25] Reactors were centrifuged for 10 min at 9000 rpm, and the isolated supernatant was then filtered to 0.45 μm to separate dissolved and adsorbed OM. This filtered supernatant was subsequently characterized in terms of pH (Text S2, Table S1 and Figure S1) and stored at 4 °C prior to further analysis(Text S1). Analytical techniques included dissolved organic carbon (DOC) analysis, inductively coupled plasma mass spectrometry (ICP-MS), and Fourier transform ion cyclotron resonance mass spectrometry (FTICR-MS). Solid-phase Fe−OM samples were freeze-dried and lightly homogenized with a mortar and pestle prior to Fourier transform infrared spectroscopy (FTIR) (Text S1).

RESULTS AND DISCUSSION

Threshold Effects of Ionic Strength on Adsorption of OM to Fh Surfaces. Adsorption of OM to Fh was most extensive in LIW, with 3.74 ± 0.36 mg C/g Fh after 24 h and in MIW with 3.24 ± 0.56 mg C/g Fh after 24 h (Figure 1). Adsorption behavior is best described by a linearized Freundlich equation (eq S1),[26] with r^2 values of 0.93 for MIW and 0.91 for LIW (Figures S2). This description of adsorption behavior assumes multilayer adsorption processes and heterogeneous adsorption sites.[26] Similar overall rates of OM adsorption were determined from fits using eqs S2 and S5: 1.8×10^{-4} mg g^{-1} min^{-1} in LIW and 1.9×10^{-4} mg g^{-1} min^{-1} in MIW (Table S2). Higher concentrations of DOM adsorbed to Fh have been reported in the absence of ions (236 mg C/g Fh at pH 4 and 200 mg C/g Fh at pH 7)[27] and in the presence of single cations, ranging from 0.1 to 10 mM (≤200 mg C/g Fh at pH 6.5).[20] In this study, C adsorption was most likely limited by the lower initial ratio of C to Fh, and the reduced chemodiversity and composition of the estuarine DOM compared to those of litter-derived DOM used in previous studies.

In contrast, the extent of adsorption of OM to Fh in the HIW matrix was significantly reduced in comparison to those in the MIW (p < 0.05) and LIW (p < 0.001) matrices, with 2.12 ± 0.03 mg C/g Fh (Figure 1). Adsorption in HIW was also described well by a linearized Freundlich equation, with an r^2 of 0.96 (Figure S2). Additionally, the overall rate of adsorption was slower, at a rate of 7.7×10^{-4} mg g^{-1} min^{-1} (Table S2). Strikingly, the pH in the HIW reactors at 24 h was 6.5, while the pH values of the MIW and LIW reactors were

https://doi.org/10.1021/acs.estlett.1c00432
Environ. Sci. Technol. Lett. 2021, 8, 719−724

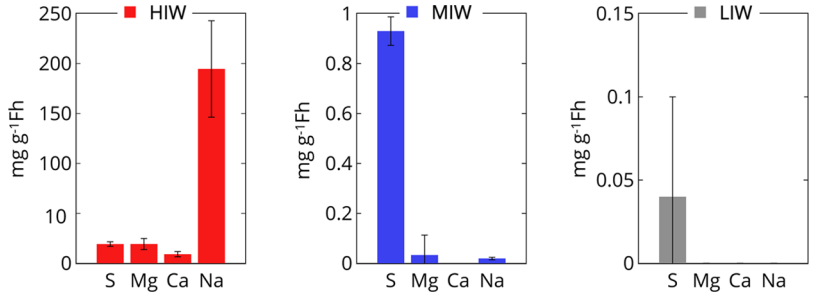

Figure 2. Concentrations adsorbed (milligrams per gram of Fh) of sulfur (S), magnesium (Mg), calcium (Ca), and sodium (Na) in solution, determined as the difference between concentrations at 1 min and at 24 h in high-ionic strength water [HIW (red)], mid-ionic strength water [MIW (blue)], and low-ionic strength water [LIW (gray)]. Concentrations were measured via inductively coupled plasma mass spectrometry, and error bars represent the standard deviation calculated from triplicate reactor concentrations.

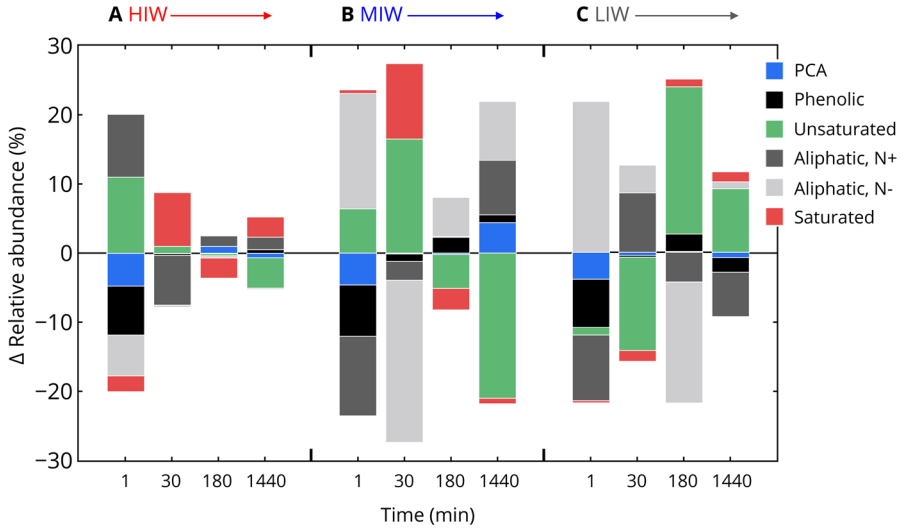

Figure 3. Changes in the relative abundance ofDOM composition induced by adsorption with Fh under (A) high-ionic strength water (HIW), (B) mid-ionic strength water (MIW), and (C) low-ionic strength water (LIW) matrices. Negative delta values (−) indicate removal from DOM solutions and sorption to mineral surfaces, while positive changes in abundance indicate the resulting enrichment in solution. Changes in relative abundances were calculated from peak-to-peak presence−absence differences between temporal reacted DOM and initial, unreacted DOM; for further details, see the Supporting Information. Composition class abbreviations are as follows: PCA, polycyclic aromatic; N+, nitrogen-containing; N-, nitrogen-less.

5.6 and 4.5, respectively. This difference in pH likely influenced the extent of C adsorption, as the Fh surface is more positively charged at lower pH (PZC = 7.5),[8,26] and carboxyl groups (pK_a = 4), important in organo−mineral complex formation,[28−30] are negatively charged. However, previous studies showed only a16% increase in litter-derived DOM adsorption at pH 4 compared to pH 7,[27] whereas in this study, a 43% increase was measured at pH 4.6 (LIW) compared to pH 6.5 (HIW). We hypothesize that pH alone would not account for such a large shift in the extent of OM adsorption and that increasing the ionic strength appears to exhibit a threshold inhibitory effect on adsorption capacity and rate.

Dynamic Ion Behavior during OM Adsorption. To probe the mechanisms that drive reduced OM adsorption in HIW matrices, aqueous ion adsorption dynamics were explored. Net changes and sorption processes were determined by calculating the difference in total S, Mg, Na, and Ca concentrations from 1 min to 24 h (Figure 2). In HIW, all four species were adsorbed to Fh, ranging from 9 to 195 mg/g Fh (Table S3). High concentrations of adsorbed ions likely limited the extent of OM adsorption, rather than enhancing adsorption, as has been previously observed in simple systems for a range of pH values.[18−20,31] Cations Mg, Ca, and Na were soluble after 24 h in LIW in comparison to 1 min (Figure 2), stemming either from dissociation with OM or from desorption from the Fh surface after rapid initial adsorption of these OM-associated cations. Only small amounts of Mg (0.033 ± 0.08 mg/g) and Na (0.019 ± 0.005 mg/g) were adsorbed in MIW (Figure 2). In MIW, after 24 h S was the most extensively adsorbed ion in the matrix, with 0.93 ± 0.06 mg S/g Fh; however, this was several orders of magnitude less than in HIW (19.2 ± 2.3 mg S/g Fh) (Table S3). Sulfate forms both inner- and outer-sphere complexes on the surface of iron minerals, depending on the pH.[32−34] Thus, in the HIW system at pH 6.5, the high concentration of adsorbed sulfate is predicted to form primarily bulky outer-sphere complexes, compared to the MIW system at pH 5.6 where a mix of inner- and outer-sphere complexes are predicted.[32] Both the high concentration and the adsorption geometry of sulfate in the HIW system could play a role in limiting OM adsorption.

Linear correlation analysis between DOC and divalent cations Ca and Mg was also performed to assess possible cation bridging mechanisms (Figure S3). DOC was inversely

https://doi.org/10.1021/acs.estlett.1c00432
Environ. Sci. Technol. Lett. 2021, 8, 719−724

correlated with aqueous Ca in LIW (r^2 = 0.64) and MIW (r^2 = 0.65) and not well correlated in HIW (r^2 = 0.38) (Figure S3). Similar relationships were observed between DOC and Mg (Figure S3). These correlation constants suggest adsorption of coastal-derived OM to Fh is not enhanced by cation bridging in complex ionic matrices. Instead, OM adsorption is likely driven by a combination of surface site availability and pH differences similar to that between freshwater and seawater. While previous studies have demonstrated an increase in OM adsorption in the presence of ≤30 mM Ca over a wide pH range (4−9),[18−20] these studies have done so in a simplified matrix that does not contain other competing cations. Although a higher extent of cation adsorption is expected at higher pH values and cation adsorption is likely inhibited at the final pH values in the MIW and LIW systems,[35] studies using single cations have demonstrated 1.6 times greater OM adsorption even at pH 4.5.[18] Therefore, we hypothesize that while Ca may enhance OM adsorption in relatively simple matrices, the complexity of high-ionic strength matrices such as seawater may inhibit this enhancement effect. We hypothesize that cations such as Mg and Na could occupy mineral surface sites similar to those of Ca (i.e., hydroxyl sites), thereby limiting Ca adsorption and the formation of bridging complexes. Additionally, Mg and Na may react with OM compounds directly and bind with functional groups that would be used in the formation of Ca−OM surface complexes.

Impact of Ionic Strength on Temporal OM Molecular Fractionation. Electrospray ionization Fourier transform ion cyclotron mass spectrometry (FTICR-MS), operating in negative ion mode, was used to analyze DOM before (denoted as "unreacted") and after reaction with Fh at select time points (1, 30, 180, and 1440 min, reaction time) to probe the effect of ionic strength on compound-selective adsorption (Figure 3 and Table S4). Selective adsorption, as expressed in Figure 3, is represented by a decrease in the total relative abundance of those compound types that result from complete peak removal from solution (Text S1). Subsequent enrichment of compounds remaining in solution and any desorption are denoted by positive changes in the relative abundance.

Adsorption to Fh under LIW conditions was notably identical to that previously observed in reactions between litter-derived DOM and goethite, despite differences in oxide solid-phase speciation and initial DOM chemodiversity.[25] We observed initial rapid adsorption of polycyclic aromatic and phenolic compounds within the first minute of reaction, followed by secondary adsorption of predominantly highly unsaturated compounds after exposure for 30 and 180 min (Figure 3C). Compounds removed from solution at equilibrium (1440 min) were primarily aliphatic moieties and likely result from nonselective binding after initial selective scaffolding.[25] Novel to this system, however, was the preferential rapid adsorption of nitrogenous aliphatic compounds under LIW and MIW conditions, suggesting that these N-bearing moieties may also be involved in direct surface complexation reactions. Previous research has found that N-rich amino sugars and amino acids are capable of directly binding reactions to diverse mineral surfaces and are enriched in mineral-associated OM fractions[25,36,37]

Adsorption under MIW conditions was similarly characterized by rapid preferential adsorption of aromatic compounds, with the greatest shift in AI_{mod} observed (Table S4). FTIR spectra of solid-phase samples at 30 and 180 min corroborate the finding that LIW and MIW solids have similar structures via hierarchal clustering analysis (HCA),[38] which are distinct from HIW samples (Figure S4). Adsorption under MIW conditions induced aliphatic moieties to bind prior to unsaturated compounds. The latter, a deviation from LIW observations, may be due to exchange between compounds, supported by C release midreaction in MIW matrices (Figure 1), or sterically induced constraints as organic compounds compete for surface area with ionic species, which were observed to be adsorbed at significant concentrations in MIW matrices (Figure 2).

In contrast, HIW DOM matrices exhibited markedly reduced levels of molecular fractionation, significant only in the first 30 min (Figure 3C and Table S4). In conjunction with observations of initial rapid C adsorption rates but lower total C adsorption (Figure 1, Table S2), a threshold effect of rapid selective adsorption in direct competition with ions for surface area is evident, in which little to no adsorption or fractionation is possible after surface saturation and ions are not facilitating OM complexation. The preferential adsorption of lower-molecular weight compounds after the first 1 min (MIW) or 30 min (LIW and HIW) of adsorption (Table S4) also suggests steric hindrance impeded temporal assembly of OM at the mineral surface. HCA of FTIR spectra showed HIW solids are distinct from LIW solids throughout but similar to MIW at later time points of 960 and 1440 min (Figure S4). Changes in unsaturated compounds that occurred in solution at later time points (Figure 3) likely contribute in part to this clustering. Similarities between the HIW and MIW solid phases at 1 min are attributed to the initial adsorption of sulfate in these matrices (Tables S3 and S5 and Figures S4−S6).

It is important to note that all reactions, regardless of matrix, resulted in a net preferential adsorption of higher oxygenation, unsaturated and high-molecular weight compounds by reaction equilibrium, as is often observed[9,10,25,27,39] (Table S4), and that these net changes do not encompass the true dynamism at play during OM adsorption, particularly under contrasting ionic strength regimes. Ionic strength affects not only the molecular fractionation of DOM onto Fh but also the extent and rate of OM adsorption, as demonstrated in this study. Somewhat unexpectedly, in complex ionic matrices (HIW and MIW), cation bridging mechanisms did not seem to enhance OM adsorption but rather induced heightened competition for the Fh surface as the ionic strength increased. In vulnerable coastal environments where SLR is expected to induce salinization and increases in ionic strength, DOM concentrations could possibly increase, and C speciation over time could dramatically change. C bioavailability and consequently potential CO_2 production in future environments could be impacted by the changes in adsorption with respect to ionic strength demonstrated in this study.

■ ASSOCIATED CONTENT

Supporting Information

The Supporting Information is available free of charge at https://pubs.acs.org/doi/10.1021/acs.estlett.1c00432.

Ferrihydrite synthesis, DOM isolation, composition of media, and dissolved species analysis including mass spectrometry data analysis; supplemental equations describing rate calculations and adsorption (eqs 1−3); tables of pH, ion concentration, and mass spectrometry data (Tables S1−S6); figures of pH, adsorption, FTIR,

https://doi.org/10.1021/acs.estlett.1c00432
Environ. Sci. Technol. Lett. 2021, 8, 719−724

and XRD data (Figures S1−S7); and additional references.

(PDF)

AUTHOR INFORMATION

Corresponding Author

E. J. Tomaszewski − *Department of Plant and Soil Science, University of Delaware, Newark, Delaware 19716, United States;* Present Address: U.S. Geological Survey, 3215 Marine St., #E141, Boulder, CO 80303; orcid.org/0000-0003-1211-7524; Phone: 303-236-2000; Email: etomaszewski@usgs.gov

Authors

E. K. Coward − *Department of Plant and Soil Science, University of Delaware, Newark, Delaware 19716, United States;* Present Address: Department of Chemistry and Biochemistry, University of California, San Diego, Urey Hall 5120, La Jolla, CA 92093.; orcid.org/0000-0002-3279-8788

D. L. Sparks − *Department of Plant and Soil Science, University of Delaware, Newark, Delaware 19716, United States*

Complete contact information is available at: https://pubs.acs.org/10.1021/acs.estlett.1c00432

Notes

The authors declare no competing financial interest.

ACKNOWLEDGMENTS

This work was funded by National Science Foundation EPSCoR Grant 1757353 and the state of Delaware. FTICR-MS analysis was performed at the COSMIC Lab at Old Dominion University, and the authors thank Drs. Isaiah Ruhl, Ravi Garimella, and Rachel Sleighter for analysis and sample calibration assitance. ICP-MS and FTIR analysis were performed in the Advanced Materials Characterization Lab at the University of Delaware with the assistance of Dr. Chin Chen Kuo. Finally, the authors thank Dr. Yu-Ping Chin for use of the TOC-L instrument.

REFERENCES

(1) Church, J. A.; Clark, P. U.; Cazenave, A.; Gregory, J. M.; Jevrejeva, S.; Levermann, A.; Merrifield, M. A.; Milne, G. A.; Nerem, R. S.; Nunn, P. D.; Payne, A. J.; Pfeffer, W. T.; Stammer, D.; Unnikrishnan, A. S. Sea Level Change. Technical Report; Cambridge University Press, 2013.

(2) Herbert, E. R.; Boon, P.; Burgin, A. J.; Neubauer, S. C.; Franklin, R. B.; Ardón, M.; Hopfensperger, K. N.; Lamers, L. P. M.; Gell, P. A Global Perspective on Wetland Salinization: Ecological Consequences of a Growing Threat to Freshwater Wetlands. *Ecosphere* **2015**, *6* (10), art206.

(3) Millero, F. J.; Feistel, R.; Wright, D. G.; McDougall, T. J. The Composition of Standard Seawater and the Definition of the Reference-Composition Salinity Scale. *Deep Sea Res., Part I* **2008**, *55* (1), 50−72.

(4) Pilson, M. E. Q. *An Introduction to the Chemistry of the Sea*, 2nd ed.; Cambridge University Press: Cambridge, U.K., 2012.

(5) Lalonde, K.; Mucci, A.; Ouellet, A.; Gélinas, Y. Preservation of Organic Matter in Sediments Promoted by Iron. *Nature* **2012**, *483* (7388), 198−200.

(6) Hiemstra, T. Surface and Mineral Structure of Ferrihydrite. *Geochim. Cosmochim. Acta* **2013**, *105*, 316−325.

(7) Michel, F. M.; Ehm, L.; Antao, S. M.; Lee, P. L.; Chupas, P. J.; Liu, G.; Strongin, D. R.; Schoonen, M. A. A.; Phillips, B. L.; Parise, J. B. The Structure of Ferrihydrite, a Nanocrystalline Material. *Science* **2007**, *316* (5832), 1726−1729.

(8) Cornell, R. M.; Schwertmann, U. *The Iron Oxides: Structure, Properties, Reactions, Occurrences and Uses*; John Wiley & Sons: Weinheim, Germany, 2006.

(9) Coward, E. K.; Ohno, T.; Plante, A. F. Adsorption and Molecular Fractionation of Dissolved Organic Matter on Iron-Bearing Mineral Matrices of Varying Crystallinity. *Environ. Sci. Technol.* **2018**, *52* (3), 1036−1044.

(10) Lv, J.; Zhang, S.; Wang, S.; Luo, L.; Cao, D.; Christie, P. Molecular-Scale Investigation with ESI-FT-ICR-MS on Fractionation of Dissolved Organic Matter Induced by Adsorption on Iron Oxyhydroxides. *Environ. Sci. Technol.* **2016**, *50* (5), 2328−2336.

(11) Xu, H.; Ji, L.; Kong, M.; Jiang, H.; Chen, J. Molecular Weight-Dependent Adsorption Fractionation of Natural Organic Matter on Ferrihydrite Colloids in Aquatic Environment. *Chem. Eng. J.* **2019**, *363*, 356−364.

(12) van Dijk, G.; Lamers, L. P. M.; Loeb, R.; Westendorp, P.-J.; Kuiperij, R.; van Kleef, H. H.; Klinge, M.; Smolders, A. J. P. Salinization Lowers Nutrient Availability in Formerly Brackish Freshwater Wetlands; Unexpected Results from a Long-Term Field Experiment. *Biogeochemistry* **2019**, *143* (1), 67−83.

(13) van Dijk, G.; Smolders, A. J. P.; Loeb, R.; Bout, A.; Roelofs, J. G. M.; Lamers, L. P. M. Salinization of Coastal Freshwater Wetlands; Effects of Constant versus Fluctuating Salinity on Sediment Biogeochemistry. *Biogeochemistry* **2015**, *126* (1−2), 71−84.

(14) Weston, N. B.; Dixon, R. E.; Joye, S. B. Ramifications of Increased Salinity in Tidal Freshwater Sediments: Geochemistry and Microbial Pathways of Organic Matter Mineralization. *J. Geophys. Res.* **2006**, *111* (G1), n/a DOI: 10.1029/2005JG000071.

(15) Weston, N. B.; Neubauer, S. C.; Velinsky, D. J.; Vile, M. A. Net Ecosystem Carbon Exchange and the Greenhouse Gas Balance of Tidal Marshes along an Estuarine Salinity Gradient. *Biogeochemistry* **2014**, *120* (1−3), 163−189.

(16) Canavan, R. W.; Slomp, C. P.; Jourabchi, P.; Van Cappellen, P.; Laverman, A. M.; van den Berg, G. A. Organic Matter Mineralization in Sediment of a Coastal Freshwater Lake and Response to Salinization. *Geochim. Cosmochim. Acta* **2006**, *70* (11), 2836−2855.

(17) Kleber, M.; Sollins, P.; Sutton, R. A Conceptual Model of Organo-Mineral Interactions in Soils: Self-Assembly of Organic Molecular Fragments into Zonal Structures on Mineral Surfaces. *Biogeochemistry* **2007**, *85* (1), 9−24.

(18) Barreto, M. S. C.; Elzinga, E. J.; Ramlogan, M.; Rouff, A. A.; Alleoni, L. R. F. Calcium Enhances Adsorption and Thermal Stability of Organic Compounds on Soil Minerals. *Chem. Geol.* **2021**, *559*, 119804.

(19) Sowers, T. D.; Stuckey, J. W.; Sparks, D. L. The Synergistic Effect of Calcium on Organic Carbon Sequestration to Ferrihydrite. *Geochem. Trans.* **2018**, *19* (1), 4.

(20) Liu, M.; Ding, Y.; Peng, S.; Lu, Y.; Dang, Z.; Shi, Z. Molecular Fractionation of Dissolved Organic Matter on Ferrihydrite: Effects of Dissolved Cations. *Environmental Chemistry* **2019**, *16* (2), 137.

(21) Wang, Y.; Zhang, Z.; Han, L.; Sun, K.; Jin, J.; Yang, Y.; Yang, Y.; Hao, Z.; Liu, J.; Xing, B. Preferential Molecular Fractionation of Dissolved Organic Matter by Iron Minerals with Different Oxidation States. *Chem. Geol.* **2019**, *520*, 69−76.

(22) Kunhi Mouvenchery, Y.; Kučerík, J.; Diehl, D.; Schaumann, G. E. Cation-Mediated Cross-Linking in Natural Organic Matter: A Review. *Rev. Environ. Sci. Bio/Technol.* **2012**, *11* (1), 41−54.

(23) Aquino, A. J. A.; Tunega, D.; Schaumann, G. E.; Haberhauer, G.; Gerzabek, M. H.; Lischka, H. The Functionality of Cation Bridges for Binding Polar Groups in Soil Aggregates. *Int. J. Quantum Chem.* **2011**, *111* (7−8), 1531−1542.

(24) Riedel, T.; Biester, H.; Dittmar, T. Molecular Fractionation of Dissolved Organic Matter with Metal Salts. *Environ. Sci. Technol.* **2012**, *46* (8), 4419−4426.

(25) Coward, E. K.; Ohno, T.; Sparks, D. L. Direct Evidence for Temporal Molecular Fractionation of Dissolved Organic Matter at the Iron Oxyhydroxide Interface. *Environ. Sci. Technol.* **2019**, *53* (2), 642−650.
(26) Sparks, D. L. *Environmental Soil Chemistry*, 2nd ed.; Academic Press: Burlington, MA, 2003.
(27) Chen, C.; Dynes, J. J.; Wang, J.; Sparks, D. L. Properties of Fe-Organic Matter Associations via Coprecipitation versus Adsorption. *Environ. Sci. Technol.* **2014**, *48*, 13751.
(28) Kleber, M.; Mikutta, R.; Torn, M. S.; Jahn, R. Poorly Crystalline Mineral Phases Protect Organic Matter in Acid Subsoil Horizons. *Eur. J. Soil Sci.* **2005**, *0* (0), 050912034650054.
(29) Kleber, M.; Eusterhues, K.; Keiluweit, M.; Mikutta, C.; Mikutta, R.; Nico, P. S. Mineral−Organic Associations: Formation, Properties, and Relevance in Soil Environments. *Adv. Agron.* **2015**, *130*, 1−140.
(30) Kaiser, K.; Guggenberger, G. The Role of DOM Sorption to Mineral Surfaces in the Preservation of Organic Matter in Soils. *Org. Geochem.* **2000**, *31* (7), 711−725.
(31) Weng, L. P.; Koopal, L. K.; Hiemstra, T.; Meeussen, J. C. L.; Van Riemsdijk, W. H. Interactions of Calcium and Fulvic Acid at the Goethite-Water Interface. *Geochim. Cosmochim. Acta* **2005**, *69* (2), 325−339.
(32) Gu, C.; Wang, Z.; Kubicki, J. D.; Wang, X.; Zhu, M. X-Ray Absorption Spectroscopic Quantification and Speciation Modeling of Sulfate Adsorption on Ferrihydrite Surfaces. *Environ. Sci. Technol.* **2016**, *50* (15), 8067−8076.
(33) Zhu, M.; Northrup, P.; Shi, C.; Billinge, S. J. L.; Sparks, D. L.; Waychunas, G. A. Structure of Sulfate Adsorption Complexes on Ferrihydrite. *Environ. Sci. Technol. Lett.* **2014**, *1* (1), 97−101.
(34) Peak, D.; Ford, R. G.; Sparks, D. L. An in Situ ATR-FTIR Investigation of Sulfate Bonding Mechanisms on Goethite. *J. Colloid Interface Sci.* **1999**, *218* (1), 289−299.
(35) Dzombak, D. A.; Morel, F. M. M. *Surface Complexation Modeling: Hydrous Ferric Oxide*; John Wiley & Sons: New York, 1990.
(36) Zimmerman, A. R.; Goyne, K. W.; Chorover, J.; Komarneni, S.; Brantley, S. L. Mineral Mesopore Effects on Nitrogenous Organic Matter Adsorption. *Org. Geochem.* **2004**, *35* (3), 355−375.
(37) Mikutta, R.; Turner, S.; Schippers, A.; Gentsch, N.; Meyer-Stüve, S.; Condron, L. M.; Peltzer, D. A.; Richardson, S. J.; Eger, A.; Hempel, G.; Kaiser, K.; Klotzbücher, T.; Guggenberger, G. Microbial and Abiotic Controls on Mineral-Associated Organic Matter in Soil Profiles along an Ecosystem Gradient. *Sci. Rep.* **2019**, *9* (1), 10294.
(38) Panchuk, V.; Yaroshenko, I.; Legin, A.; Semenov, V.; Kirsanov, D. Application of Chemometric Methods to XRF-Data − A Tutorial Review. *Anal. Chim. Acta* **2018**, *1040*, 19−32.
(39) Young, R.; Avneri-Katz, S.; McKenna, A.; Chen, H.; Bahureksa, W.; Polubesova, T.; Chefetz, B.; Borch, T. Composition-Dependent Sorptive Fractionation of Anthropogenic Dissolved Organic Matter by Fe(III)-Montmorillonite. *Soil Systems* **2018**, *2* (1), 14.

https://doi.org/10.1021/acs.estlett.1c00432
Environ. Sci. Technol. Lett. 2021, 8, 719−724